Technical Report No. 2

to the

Office of Naval Research

Contract N00014-67-A-0117-0010, NR 031-745

THE EFFECTS OF GROWTH SPEED AND HEAT TREATMENT ON DEFORMATION OF ALIGNED Ag_3Mg-AgMg AND Al-Ag_2Al EUTECTICS

R. H. Bellows, Y. G. Kim and N. S. Stoloff

Materials Division

Rensselaer Polytechnic Institute

Troy, New York 12181

August 31, 1972

37

Unclassified
Security Classification

DOCUMENT CONTROL DATA - R & D

(Security classification of title, body of abstract and indexing annotation must be entered when the overall report is classified)

1. ORIGINATING ACTIVITY (Corporate author)
Materials Division
Rensselaer Polytechnic Institute
Troy, New York 12181

2a. REPORT SECURITY CLASSIFICATION
Unclassified

2b. GROUP

3. REPORT TITLE
THE EFFECTS OF GROWTH SPEED AND HEAT TREATMENT ON DEFORMATION OF ALIGNED Ag_3Mg AND Al-Ag_2Al EUTECTICS

4. DESCRIPTIVE NOTES (Type of report and inclusive dates)
Technical Report No. 2

5. AUTHOR(S) (First name, middle initial, last name)
Y. G. Kim R. H. Bellows
N. S. Stoloff

6. REPORT DATE	7a. TOTAL NO. OF PAGES	7b. NO. OF REFS
August 31, 1972	23	20

8a. CONTRACT OR GRANT NO
N00014-67-A-0117-0010

b. PROJECT NO
NR031-745

c.

d.

9a. ORIGINATOR'S REPORT NUMBER(S)

9b. OTHER REPORT NO(S) (Any other numbers that may be assigned this report)

10. DISTRIBUTION STATEMENT
Reproduction in whole or in part is permitted for any purpose of the United States Government.

11. SUPPLEMENTARY NOTES

12. SPONSORING MILITARY ACTIVITY
Office of Naval Research
Department of the Navy
Arlington, Virginia 22217

13. ABSTRACT

Tensile properties of aligned Ag_3Mg-AgMg and Al-Ag_2Al eutectics have been determined as a function of growth speed at temperatures between -196°C and 300°C. Strength of Ag_3Mg-AgMg increases with decreasing spacing, λ, at all test temperatures, but the strength of Al-Ag_2Al is more dependent on eutectic grain size. Ordering of the Ag_3Mg phase increases the effectiveness of interphase boundaries as barriers to slip and increases the strength of Ag_3Mg-AgMg. Aging treatments to produce γ' in the Al-rich phase markedly increases strength of Al-Ag_2Al. Fracture behavior of both alloys is discussed.

DD FORM 1 NOV 68 1473

Unclassified
Security Classification

14 KEY WORDS	LINK A		LINK B		LINK C	
	ROLE	WT	ROLE	WT	ROLE	WT
Silver-Magnesium Alloys						
Eutectic Composite						
Long-Range Order						
Unidirectional Solidification						
Silver-Aluminum Alloys						
Eutectic grain size						
Fracture mechanisms						

THE EFFECTS OF GROWTH SPEED AND HEAT TREATMENT ON DEFORMATION OF ALIGNED Ag_3Mg-AgMg AND Al-Ag_2Al EUTECTICS

R. H. Bellows, Y. G. Kim and N. S. Stoloff
Rensselaer Polytechnic Institute
Troy, New York 12181

Abstract

The tensile properties of aligned Al-Ag_2Al and Ag_3Mg-AgMg eutectics were studied as functions of growth speed, post-solidification heat treatments and test temperature. The yield and ultimate strengths of the latter were markedly altered by thermal treatments which produced long-range order in the Ag_3Mg phase. The strength of Al-Ag_2Al was altered by heat treatments which induced precipitation in the aluminum-rich phase. The dependence of yield strength on interlamellar spacing, λ, was markedly different for the two alloys. For the Ag-Al system, strength decreased with decreasing λ but increased with finer eutectic grain size, d, brought about by slower solidification rates. The Ag-Mg alloy, on the other hand, revealed the more typical increase in strength with $\lambda^{-\frac{1}{2}}$; there was a pronounced increase in slope of σ_y vs $\lambda^{-\frac{1}{2}}$ when the Ag_3Mg phase exhibited long range order. The influence of test temperature on yield strength, UTS and fracture elongation was determined for both alloys. Fracture mechanisms were studied by transmission and scanning electron microscopy.

INTRODUCTION

Previous studies (1-3) have shown that higher strengths of aligned eutectics are achieved for rapid growth rates (small interlamellar spacings) and for samples with few growth faults which are tested parallel to the growth direction. Recent work has shown that additional strengthening may be introduced by post-solidification heat treatments to produce either a fine precipitate distribution, (Al-$CuAl_2$ system) (4) or to induce long range order (AgMg-Ag_3Mg system) (5) in one of the co-existing phases. It is the purpose of this paper to present additional information concerning the influence of ordering heat treatments on mechanical behavior in the AgMg-Ag_3Mg system, and to contrast the behavior of this alloy with a non-ordering Al-Ag_2Al eutectic.

The experimental program consisted of producing directionally solidified samples of each alloy at several growth rates, performing post-solidification heat treatments, and determining the tensile properties as a function of test temperature in the range -196°C to 300°C.

ALLOY STRUCTURE AND CRYSTALLOGRAPHY

The Ag-33.6a%Mg (nominal) eutectic forms at 759°C and consists of 40v% of the ordered CsCl type phase AgMg, and 60v% of a solid solution of approximate composition Ag-27a%Mg (6). AgMg is ordered to its melting point of 820°C, while Ag-27%Mg undergoes an ordering reaction from disordered fcc to a fct DO_{23} type superlattice below about 375°C (7). A preliminary report of tensile behavior of this system has recently been published (5). No data are available, however, concerning crystallographic relations between the co-existing phases.

Al-37.5a%Ag forms a eutectic at 566°C between an fcc aluminum-rich solid solution and an hcp intermetallic phase corresponding in composition to off-stoichiometric

Ag_2Al (6). The continuous Ag_2Al phase is present in 53v%. The composition of the intermetallic phase is reduced only from 42 to 40a%Al on cooling from 566°C to room temperature. However, the alpha solid solution varies in composition from 23.8a%Ag at the melting point to less than a fraction of a percent Ag at room temperature. This offers the possibility of employing post-solidification heat treatments to induce precipitation in the quenched alpha solid solution. Previous work on this eutectic system has been confined to studying the growth characteristics of the eutectic, (8,9) and the crystallographic relationships between the phases (9,10). Elwood and Bagley (10) report $(111)_{Al}//(0001)_{Ag_2Al}$, and that the growth direction (which generally is not parallel to interphase boundaries) is <001>. This alloy reveals a pronounced tendency for structural breakdown of lamellae to rods, particularly at colony boundaries, as will be discussed later. Although Elwood and Bagley reported that the aluminum-rich phase is the continuous phase, the present work indicates that Ag_2Al is continuous.

EXPERIMENTAL PROCEDURE

Material Preparation

Starting materials for the two alloys were 99.999%Ag and Al and 99.995%Mg. One in. diameter ingots were melted in graphite crucibles under flowing argon in an induction unit. A shift in comparison from Ag-33.6a%Mg to Ag-32.2%Mg was necessary to remove proeutectic magnesium. Ag-Al ingots were remelted and cast into smaller ½ in. diameter ingots, unidirectionally solidified and hot swaged at 430°C to 3/16 in. diameter. The initial directional solidification before swaging proved to be a necessary step to avoid cracking during subsequent hot working. Ag-Mg on the other hand, could be hot swaged to 3/16 in. diameter directly after initially casting to 1 in. diameter.

An ingot of Al-16%Ag also was prepared to permit studies of age hardening effects in the aluminum-rich phase of the Ag-Al eutectic.

Directional Solidification

Samples of each eutectic alloy were directionally solidified in graphite crucibles inside a resistance-wound Bridgeman apparatus through which argon was flowing. The crucible was withdrawn from the furnace, through a water-cooled collar, at a rate which could be varied from 0.42 to 500 cm/hr. Good alignment without horizontal banding could be obtained in the Ag-Al alloy only for rates between 1.73 and 13.85 cm/hr. Ag-Mg was much easier to grow, good alignment being achieved for any rate below 175 cm/hr. A breakdown to colony structure occurred at higher rates. The structure of Ag-Mg ingots selected for study always consisted of aligned plates parallel to the growth direction, Fig. 1a). Ag-Al, on the other hand, while predominantly lamellar, often exhibited clusters of rods at eutectic grain boundaries, as shown in Fig. 1b). Ingots containing a large proportion of such rods was discarded. Longitudinal sections confirmed the reported off-axis growth of many eutectic grains in this system (8-10).

The relationship between average plate spacing $\lambda = t_1 + t_2$, (where t_1 and t_2 are the thickness of adjacent lamellae of the two phases), and growth rate, R, is shown in Fig. 2. Both alloys obey the relation $\lambda^2 R = \text{const.}$, where the constant = 7.4×10^{-11} cm^3/sec for Ag-Al and 1.5×10^{-9} cm^3/sec for Ag-Mg*.

*Note: In an earlier paper (5) λ was defined as $\frac{t_1 + t_2}{2}$. To facilitate comparison with data in the literature, the present notation was adopted.

The eutectic grain size, d, also was measured as a function of growth rate. For Ag-Al, Fig. 2, the average value of d increased with increasing growth rate, although considerable scatter was noted, as evidenced by the ranges recorded at each speed. Ag-Mg, however, exhibited little variation in grain size over the range of growth speeds employed; the average value of d was about 0.06 cm.

Specimen Preparation and Testing

After unidirectional solidification, cylindrical tensile samples with 1.25 cm gage length, 0.31 cm dia., and 0.62 cm fillet radius were machined parallel to the growth direction with a series 10-67 "Tensilkut" machine and a "Tensilathe" attachment.

Samples of Ag-Mg in which long-range order was desired in the silver-rich phase were annealed in vacuum at 500°C for 1 hour and then slow cooled to 370°C, held for 15 hours, and cooled to room temperature over a period of 10 hours. Samples in which the silver-rich phase were to be disordered were quenched after a 1 hour vacuum anneal at 500°C. This treatment disordered only the Ag-27%Mg phase; complete long range order is retained in the AgMg phase.

Two sets of post-solidification heat treatment schedules were followed for Ag-Al samples. One group of samples was stress relieved for two hours at 200°C and air cooled. The other set was annealed at 525°C for 2 hours, water quenched, and then aged at 165°C for 5 hours followed by a second water quench. The purpose of the latter treatment was to induce strengthening in the aluminum-rich phase through precipitation of γ' Ag_2Al (11).

Prior to tensile testing, gage sections of Ag-Mg were polished with Linde A and B. Ag-Al samples were electropolished-etched in a solution of 20% perchloric acid in ethanol which was held at 3-10°C by means of an ice water bath. Etching was carried out at 11 volts for 3 minutes; the samples were then rinsed in ethanol.

Tensile tests were conducted on an Instron machine at a constant strain rate of 3.3×10^{-4} sec^{-1}. Low temperature tests were performed in liquid nitrogen. Elevated temperature tests were performed under flowing argon in a resistance furnace.

Fractured tensile samples were examined by scanning electron microscopy, or two-stage plastic replicas were taken from the fracture surfaces. Replicas were shadowed with chromium at 45°, and then backed with carbon at 90°. Some fracture surfaces were coated with Epon 828 Epoxy for protection; the samples were then mounted longitudinally so that crack paths could be examined.

EXPERIMENTAL RESULTS

Ag_3Mg-AgMg

Unlike eutectic systems which contain a very strong phase in a relatively weak matrix, the aligned Ag-Mg alloy undergoes yielding with an abrupt change from elastic to plastic flow. Apparently both phases undergo plastic deformation at similar stress levels.

We have recently reported that the strength and strain hardening rate are increased and elongation is reduced by long range order in the Ag_3Mg phase (5). Of particular interest was the observation that the slope, k_λ, as is recorded in a plot of yield stress vs $\lambda^{-\frac{1}{2}}$, at room temperature was increased some 74%, Fig. 4. We have now extended

our observations to two other temperatures, -196°C and 300°C, and these data also are included in Fig. 4. There is a 93% increase in k_λ with order at -196°C, and a 37% increase at 300°C, see Table I. We note from Fig. 4 that the strength of the alloy in both ordered and disordered conditions is a sensitive function of temperature for a constant growth speed, but that k_λ at -196°C and 25°C are nearly the same for each heat treatment condition, see Table I. This indicates no difference in the effectiveness of the barriers to slip between those temperatures. However, the slopes decrease sharply at 300°C, and there is a much smaller difference between k_λ values for the two heat treatment conditions. This diminution of the apparent effectiveness of the ordering heat treatment on strength at elevated temperatures has previously been attributed to re-ordering of the disordered Ag_3Mg phase (5).

Table II is a comparison of room temperature tensile properties of as-cast Ag-Mg with aligned samples grown at two growth speeds. The as-cast material is comparable to the samples grown at 3.9 cm/hr in yield strength and in response to the ordering treatment, but the ductility in both ordered and disordered conditions is lower than for aligned material. While the eutectic is capable of appreciable plastic deformation in all conditions, ordering does decrease plasticity. There is only a small increase in elongation at temperatures to 300°C for either heat treatment condition. There was at least as great a variation in elongation with growth speed at any given temperature.

Fig. 5 shows a longitudinal section of an ordered sample grown at 3 cm/hr and tested at 25°C. The primary crack runs at angles of 30-45° to the tensile axis and to individual lamellae. As a consequence of irregularities in the structure the crack front appears to run parallel to lamellae for short distances, and then traverses other lamellae. Ordered samples, particularly those tested at -196°C, exhibit somewhat more evidence of interphase decohesion than disordered samples, as shown in the scanning electron micrograph of Fig. 6a), although the overall crack path is similar at -196°C and 25°C. Most fracture surfaces exhibited dimples of diameter approximately equal to the width of individual lamellae, as shown in Fig. 6a) and in the replica fractographs of Figs. 6b and c). The ordered sample shown in Fig. 6c) exhibits somewhat flatter fracture facets and smaller dimples than does the disordered specimen, Fig. 6b). All of these observations are consistent with the lowered ductility arising from long range order. Fig. 6a) also shows a short segment of crack running along a eutectic grain boundary, marked G. Al-Ag_2Al showed somewhat more tendency for grain boundary cracking, as will be discussed later.

TABLE I

Effects of Temperature and Order on k_λ

Temperature °C	Condition	k_λ $kg/mm^{3/2}$	Increase %
-196°C	ordered	1.58	93
-196°C	disordered	0.82	--
25°C	ordered	1.45	73
25°C	disordered	0.84	--
300°C	ordered	0.59	37
300°C	disordered	0.43	--

TABLE II

Comparison of Properties of As-Cast Ag_3Mg-AgMg with Aligned Structure

Growth Conditions	σ_y ksi	UTS ksi	ε_F %
as-cast - 0	47.8	67.0	13
as-cast - D	34.2	60.3	30.5
3.9 cm/hr - 0	48.1	75.8	22
3.9 cm/hr - D	38.8	56.8	60
15 cm/hr - 0	41.3	80.5	26
15 cm/hr - D	36.1	58.2	38.5

Al-Ag_2Al

This alloy yields in a manner similar to the Ag-Mg eutectic in that an abrupt transition occurs from elastic to plastic behavior.

Fig. 7 shows the variation in yield stress of stress-relieved Ag-Al as a function of λ for two test temperatures, 25°C and -196°C. At both temperatures yield stresses decreased with finer spacing (higher growth speeds). This is the reverse of the usual trend in strength with spacing at low temperatures for aligned eutectics (2,12,13).

Walter and Cline (12) have noted that the NiAl-Cr eutectic exhibits decreasing strength with more rapid growth speeds at 800°C ($0.86T_m$) as a consequence of the shear of eutectic grain boundaries; at 600°C the alloy behaved in the normal manner, that is, strength increased with decreasing λ. Room temperature is about $0.36T_m$ and -196°C is about $0.09T_m$ for Al-Ag_2Al, so that it is highly unlikely that cell boundary or interphase boundary shear is the explanation for the data of Fig. 7. Rather, we believe that the variation in eutectic grain size with growth rate, Fig. 3, is responsible for the observed changes in flow stress with solidification rate. As shown in Fig. 8, the yield stress at 25°C varies with the inverse square root of grain size, $d^{-\frac{1}{2}}$, in the manner of the Hall-Petch relation; at 150°C ($0.5T_m$), there is virtually no effect of grain size on strength. This suggests that the primary barriers to plastic flow at low temperatures in this alloy are the grain boundaries rather than the interphase boundaries. Some evidence to support this hypothesis is provided by observations of slip bands on samples deformed by indentation in the vicinity of grain boundaries. Fig. 9 shows slip lines which are continuous across interphase boundaries, but do not cross the grain boundaries. We shall return to this point in the Discussion.

The data shown in Figs. 7 and 8 for stress relieved material served as a baseline for further heat treatment studies. It was established from work on a heat of Al-16w%Ag (approximating the average composition of the Al-rich phase between the eutectic temperature and 25°C) that precipitation hardening occurs at 165°C after solution treatments at 525°C. A double peak in tensile strength was noted with time, as is characteristic of Al-Ag alloys (11). The first peak occurred at 5 hours, with a yield stress of 22,000 psi compared to 17,200 psi for solution treated material. Accordingly, a set of Ag-Al eutectic samples was solution treated at 525°C for 2 hours, water quenched and aged at 165°C for 5 hours. A striking increase in the room temper-

ature strength of the eutectic relative to stress relieved material was noted for all growth speeds, as shown in Fig. 10, but the anamolous dependence of strength on interphase spacing was altered only slightly, indicating no change in the primary mechanism of plastic flow. The average increment in strength of 25,000 psi for the eutectic with the aging treatment is many times larger than the modest increment in strength of 4800 psi which had been imparted to Al-16w%Ag after an identical aging treatment.

Data for recrystallized Al-Ag_2Al, summarized in Table III, indicate that no strength advantage is achieved by directional solidification of this alloy (Fig. 10), even with the aging treatment.

Nevertheless, in view of the considerable improvement in strength achieved by the aging treatment, all subsequent experimental work on the aligned eutectic was done on material which received this treatment. The influence of test temperature on the mechanical behavior of the Ag-Al eutectic, for a growth speed of 3.47 cm/hr, is summarized in Fig. 11. Load displacement curves, Fig. 11a), reveal the abrupt yielding previously referred to, as well as the extensive plasticity associated with this alloy. Fig. 11b) is a summary of yield stress, ultimate tensile stress and total elongation derived from the load displacement curves. A rapid decrease in both yield and tensile stresses occurs at temperatures above 100°C. Also, the ductility begins to increase rapidly between room temperature and 100°C. Note from Figs. 11a) and b) that there is virtually no strain hardening above 200°C.

The fracture behavior of Al-Ag_2Al was only peripherally different from that of Ag_3Mg-AgMg. Necking occurred only at temperatures above 200°C. Elliptical distortion of specimen cross sections occurred at lower temperatures, except at -196°C, where failure occurred prior to such distortion. Crack paths tended to lie between 30 and 60° to the tensile axis, Fig. 12a), with secondary cracks which followed colony or interphase boundaries lying nearly parallel to the tensile axis. The pronounced tendency for off-axis growth of eutectic grains made it possible for a single, nearly flat crack front to sometimes run along interphase boundaries, and elsewhere to run nearly perpendicular to individual lamellae. A region of predominantly transverse failure is shown in Fig. 12b). A particularly clear example of interlamellar failure is shown in Fig. 12c). Scanning electron microscopy revealed that interlamellar failure was accompanied by dimple formation, Fig. 12d). Note the change in crack appearance at the eutectic grain boundary, G, in Fig. 12d). It is apparent from this micrograph, and Fig. 12b) that cracks tend to run for short distances along interphase boundaries (or a path parallel to the boundaries) and then switch over to a path at 90° to those boundaries. For the latter path, dimples were rarely observed; instead, individual lamellae appeared to cleave, as noted by nearly featureless regions in Fig.

TABLE III

Strength of Recrystallized Al-Ag_2Al Eutectic at 25°C

Heat Treatment*	Grain Size μ	σ_y ksi	σ_{UTS} ksi
525°C - 2 hrs, W.Q.	11.5	62.2	85.5
525°C - 6 hrs, W.Q.	11.5	64.9	90.7
525°C - 20 hrs, W.Q.	19.9	60.6	84.0

*All samples re-annealed at 165°C for 5 hours.

12d). An exception to this behavior was noted when cracks intersected the clusters of rods which were shown in Fig. 1b). The fracture surface was then covered with an array of deep, equiaxed dimples. There was little effect of test temperature on the fracture mechanisms of this alloy.

DISCUSSION

Both eutectics are somewhat unusual in that the co-existing phases deform plastically from the onset of yielding, rather than the more typical elastic-plastic deformation of most eutectic and artificial composites. While it is not possible to achieve dramatic strengthening relative to the as-cast or worked and recrystallized microstructures as in many previously studied eutectics, these alloys are quite ductile under most conditions and we have shown that post-solidification heat treatments offer substantial improvements in strength, with little sacrifice of ductility. More importantly, this work has shed considerable light upon the effectiveness of several of the following proposed mechanisms of barrier strengthening in eutectic composites:

a) Modulus differences, ΔG between two co-existing phases may give rise to an image force barrier at the interphase boundary of magnitude (3):

$$\tau_{\Delta G} = \frac{\Delta G}{8\pi} \qquad (1)$$

b) A difference in lattice parameter between the phases on either side of the interface must be taken up by interface dislocations; the latter interact with slip dislocations, requiring a stress (13):

$$\tau_{\Delta b} = \frac{G\Delta b}{2\pi b} \qquad (2)$$

c) Inter-phase boundaries may act as barriers to slip in the same manner as grain boundaries, provided that slip planes and directions are not parallel across the boundary (2). In that case, by analogy to grain boundary effects (14):

$$k_\lambda = m^2 \tau_c r^{\frac{1}{2}} \qquad (3)$$

where m is an orientation factor, τ_c is the stress necessary to activate dislocations across an interphase boundary and r is a dislocation source distance.

Calculations of lattice and modulus misfit stresses for the two alloys are summarized in Table IV. In each case, G or b is taken for the continuous phase. For Al-Ag_2Al, we have had to use modulus data for pure aluminum (18), so that the modulus misfit stress for Ag-Ag_2Al is probably overestimated; also, although basal slip is the more likely deformation mode in Ag_2Al (16), we have had to use the only available modulus data, for prism slip (17). The results for Ag-Ag_2Al show that both the modulus and lattice parameter mismatch stresses are low, 4,600 and 22,600 psi, respectively, and therefore interlamellar boundaries are unlikely to offer strong barriers to plastic flow by either of these mechanisms. Since slip planes in the two phases also are coincident, it is clear that the only effective barriers to slip propagation in this eutectic are the grain boundaries and the results of Figs. 7 and 8 can then be easily understood. However, we are unable to explain the observation that grain size decreases with decreasing growth rate. An <u>increase</u> in colony size with decreasing

TABLE IV

Calculation of Barrier Stresses

Phase	b	G		$\tau_{\Delta b}$	$\tau_{\Delta G}$
	A°	10^6psi		10^3psi	10^3psi
Al-Ag	2.86	3.62*	}	4.6	22.6
Ag_2Al	2.88	4.19**			
Ag_3Mg(d)	2.92	5.8	}	19.0	127
AgMg	2.86	2.61	}	19.0	146
Ag_3Mg(o)	2.917	6.1			

* data for pure Al
**prism slip - no data available for basal slip

growth rate has previously been reported for Al-Cu eutectic (20).

For Ag_3Mg-AgMg, equally enlightening results are obtained from consideration of Table IV. (The moduli of Ag_3Mg and AgMg were obtained from (7) and (19) respectively). Modulus misfit stresses are very high, and could give rise to the large k_λ in the disordered condition. However, ordering produces only a small increase in $\tau_{\Delta G}$, some 19,000 psi, and therefore cannot explain the large increase in k_λ at low temperatures shown in Fig. 4 and Table I. The situation is even more striking with respect to lattice misfit. There is no increase in $\tau_{\Delta b}$ with order, since the lattice parameter of Ag_3Mg is virtually unchanged (15), nor is $\tau_{\Delta b}$ high enough to explain k_λ for the disordered alloy. These calculations therefore support our previous conclusion (5) that the 73% <u>increase</u> in k_λ with order at room temperature is associated with more difficult propagation of slip within the Ag_3Mg phase. Work on bulk Ag-27%Mg has indicated an 85% increase in τ_c with order, more than sufficient to explain the increase in k_λ according to Equation (3). At 300°C slip propagation becomes easier in both phases, thereby lowering τ_c and explaining the drop in k_λ relative to 25°C, see Table I. However, the disordered phase can re-order during test so that the difference in k_λ with order decreases sharply.

The value of k_λ for disordered Ag_3Mg-AgMg at 25°C, 0.84 kg/mm$^{3/2}$, is very close to that observed for lamellar Ag-Cu, 0.8 kg/mm$^{3/2}$(13). Since $\tau_{\Delta G}$ for Ag_3Mg-AgMg is 127,000 psi (Table IV), and $\tau_{\Delta G}$ and $\tau_{\Delta b}$ were both of the order of 100,000 psi for Ag-Cu (13) there is considerable support for previous suggestions (2,13) that barriers to plastic flow must be overcome by stresses arising from dislocation pileups, the length of which are limited by the interlamellar spacing.

Bertorello and Biloni (4) have studied post-solidification age hardening effects in the Al-$CuAl_2$ eutectic. They found that in the absence of aging, flow stress increased about 60% for an order of magnitude decrease in λ, although there was not a precisely linear dependence of strength on $\lambda^{-\frac{1}{2}}$. However, aged material revealed no effect at all of λ on strength. This indicated that the precipitation effect outweighed any variation of strength with spacing. Increases in ultimate tensile strength in excess of 100% were sometimes noted at a constant λ, although strength for aged material varied randomly with λ. The present work confirms the effectiveness of aging in increasing strength, although the strength-spacing relationships are different.

Finally, we shall consider the role of perfection of aligned microstructure on mechanical properties. Colony structures consist of lamellae (or rods) which are curved and not oriented along the primary growth direction. Colony structures are generally considered to be weak, and this was confirmed in the present work. Growth speeds above 175 cm/hr for Ag_3Mg-AgMg, corresponding to $\lambda^{-\frac{1}{2}} > 0.6\mu^{-\frac{1}{2}}$, resulted in no increase in strength, see Fig. 4, even though the average interlamellar spacing within the colony boundaries decreased. For Al-Ag_2Al, which was more susceptible to general structural breakdown at all growth speeds, the introduction of a colony structure caused considerable scatter in experimental results.

SUMMARY AND CONCLUSIONS

1. Both Al-Ag_2Al and Ag_3Mg-AgMg obey the relation $\lambda^2 R$ = constant.

2. The strength of Ag_3Mg-AgMg increases with $\lambda^{-\frac{1}{2}}$ at -196°C, 25°C and 300°C. The dependence of strength on λ increases sharply at -196°C and 25°C with ordering of the Ag_3Mg phase.

3. The increase in k_λ with order for Ag_3Mg-AgMg arises from increased difficulty of propagating slip in the Ag_3Mg phase.

4. The low temperature strength of Al-Ag_2Al is controlled primarily by the eutectic grain size.

5. Fracture mechanisms do not vary significantly with test temperature for either alloy, but long range order reduces the ductility of Ag_3Mg-AgMg.

ACKNOWLEDGEMENTS

This research was supported by the Office of Naval Research under Contract N00014-67-A-0117-0010, NR031-745.

REFERENCES

1. R. W. Hertzberg, F. D. Lemkey and J. A. Ford, Trans. Met. Soc. AIME, Vol. 233, 342 (1965).

2. B. J. Shaw, Acta Met., Vol. 15, 1169 (1967).

3. H. E. Cline and D. F. Stein, Trans. Met. Soc. AIME, Vol. 245, 841 (1969).

4. H. R. Bertorello and H. Biloni, Met. Trans., Vol. 3, 73 (1972).

5. Y. G. Kim and N. S. Stoloff, Met. Trans., Vol. 3, 1391 (1972).

6. M. Hansen and K. Anderko, Constitution of Binary Alloys, McGraw-Hill, New York (1958).

7. A. Gangulee and M. B. Bever, Trans. Met. Soc. AIME, Vol. 242, 278 (1968).

8. D. J. S. Cooksey, D. Munson, M. P. Williamson and A. Hellawell, Phil. Mag., 10, 745 (1964).

9. R. W. Kraft, F. D. Lemkey, D. L. Albright and F. D. George, United Aircraft Res.

Labs Rept. A-110069-5 (1962).

10. E. C. Elwood and K. Q. Bagley, J. Inst. Met., Vol. 76, 631 (1949).

11. R. B. Nicholson and J. Nutting, Acta Met., Vol. 9, 332 (1961).

12. J. L. Walter and H. E. Cline, Met. Trans., Vol. 1, 1221 (1970).

13. H. E. Cline and D. Lee, Acta Met., Vol. 18, 315 (1970).

14. R. W. Armstrong, J. Codd, R. M. Douthwaite and N. J. Petch, Phil. Mag., Vol. 7, 45 (1965).

15. L. M. Clareborough and J. F. Nicholas, Aust. J. Sci. Res., Vol. A3, 284 (1950).

16. J. D. Mote, K. Tanaka and J. E. Dorn, Trans. Met. Soc. AIME, Vol. 221, 858 (1961).

17. A. Rosen, J. D. Mote, and J. E. Dorn, Trans. Met. Soc. AIME, Vol. 230, 1070 (1964).

18. S. Howe, B. Liebmann and K. Lucke, Acta Met., Vol. 9, 625 (1961).

19. A. K. Mukherjee and J. E. Dorn, Trans. Met. Soc. AIME, Vol. 230, 1065 (1964).

20. P. K. Rohatgi and C. M. Adams, Jr., Trans. Met. Soc. AIME, Vol. 236, 1609 (1969)

FIGURE CAPTIONS

1. Transverse sections of aligned eutectic alloys a) Ag_3Mg-AgMg, R = 3.4 cm/hr, x250 b) Al-Ag_2Al, R = 1.7 cm/hr, x750 (note rods at arrows).

2. Effect of growth speed, R, on interlamellar spacing, λ.

3. Influence of growth speed on eutectic grain size, d, of Al-Ag_2Al. Bands denote scatter at each speed.

4. Dependence of yield stress on $\lambda^{-\frac{1}{2}}$ for ordered and disordered Ag_3Mg-AgMg at -196°C, 25°C and 300°C. (Points at 300°C omitted for clarity).

5. Longitudinal section, showing crack path in ordered Ag_3Mg-AgMg, R = 3 cm/hr, tested at 25°C, x500.

6. Electron fractographs of Ag_3Mg-AgMg, a) SEM, ordered, R = 13.9 cm/hr, -196°C. G denotes eutectic grain boundary. b) replica, disordered, R = 27.8 cm/hr, 25°C c) replica, ordered, R = 27.8 cm/hr, 25°C.

7. Dependence of yield stress on $\lambda^{-\frac{1}{2}}$ for stress-relieved Al-Ag_2Al at -196°C and 25°C.

8. Dependence of yield stress on $d^{-\frac{1}{2}}$ for stress-relieved Al-Ag_2Al at 25°C and 150°C.

9. Slip bands in Al-Ag_2Al, R = 6.9 cm/hr, x750. Note traces terminate at grain boundaries, G.

10. Effect of aging heat treatment on the yield strength of Al-Ag_2Al.

11. Tensile properties of aged Al-Ag_2Al a) Load-strain curves at several test temperatures b) Influence of temperature on strength and ductility.

12. Fracture modes in Al-Ag_2Al, with eutectic grain boundaries marked G. a) Crack path, -196°C, R = 31.7 cm/hr, x121 b) Lamellae fractures, -196°C, R = 3.5 cm/hr, x500 c) Interlamellar crack, -196°C, R = 6.9 cm/hr, x250 d) SEM fractograph, -196°C, R = 3.5 cm/hr, x725.

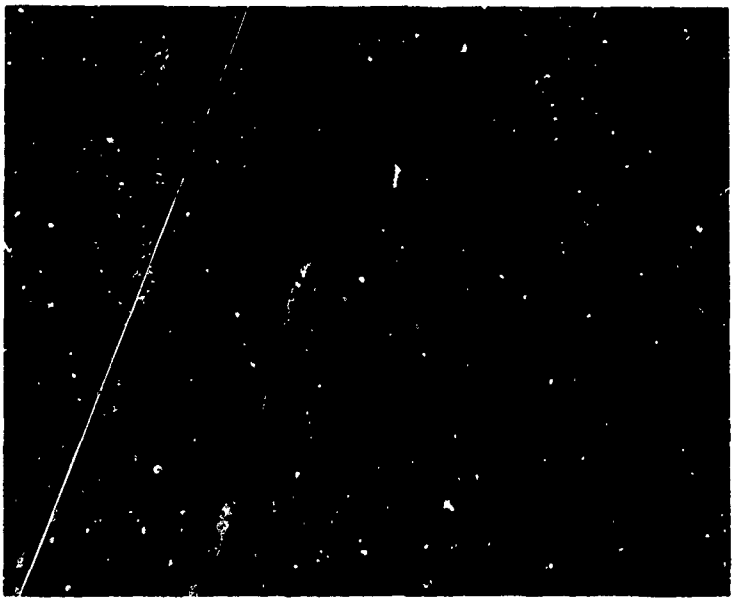

(a)

(b)

Fig. 1: Transverse sections of aligned eutectic alloys
a) Ag_3Mg-AgMg R = 3.4 cm/hr, x250
b) Al-Ag_2Al, R = 1.7 cm/hr, x750 (note rods at arrows).

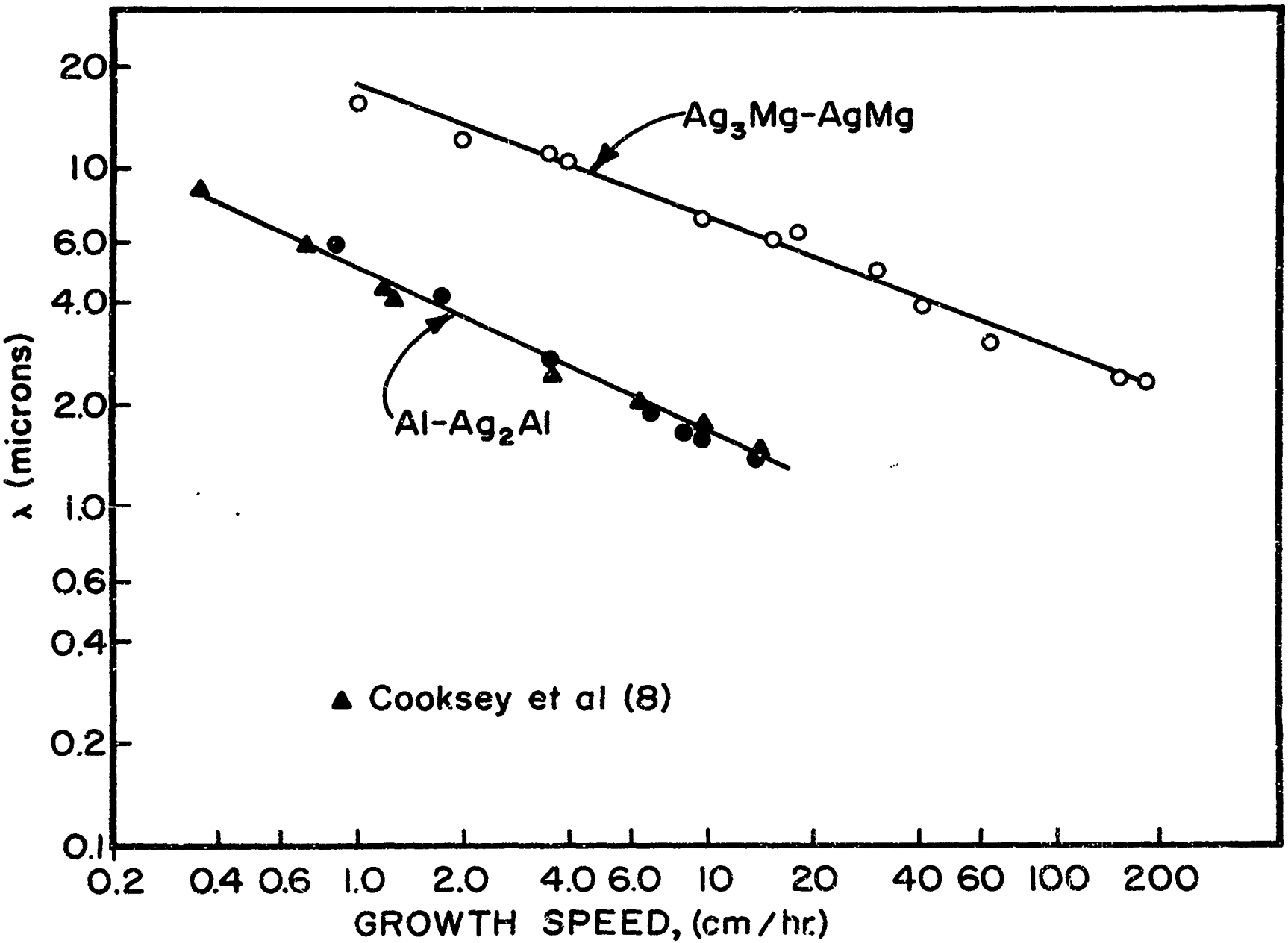

Fig. 2: Effect of growth speed, R, on interlamellar spacing, λ.

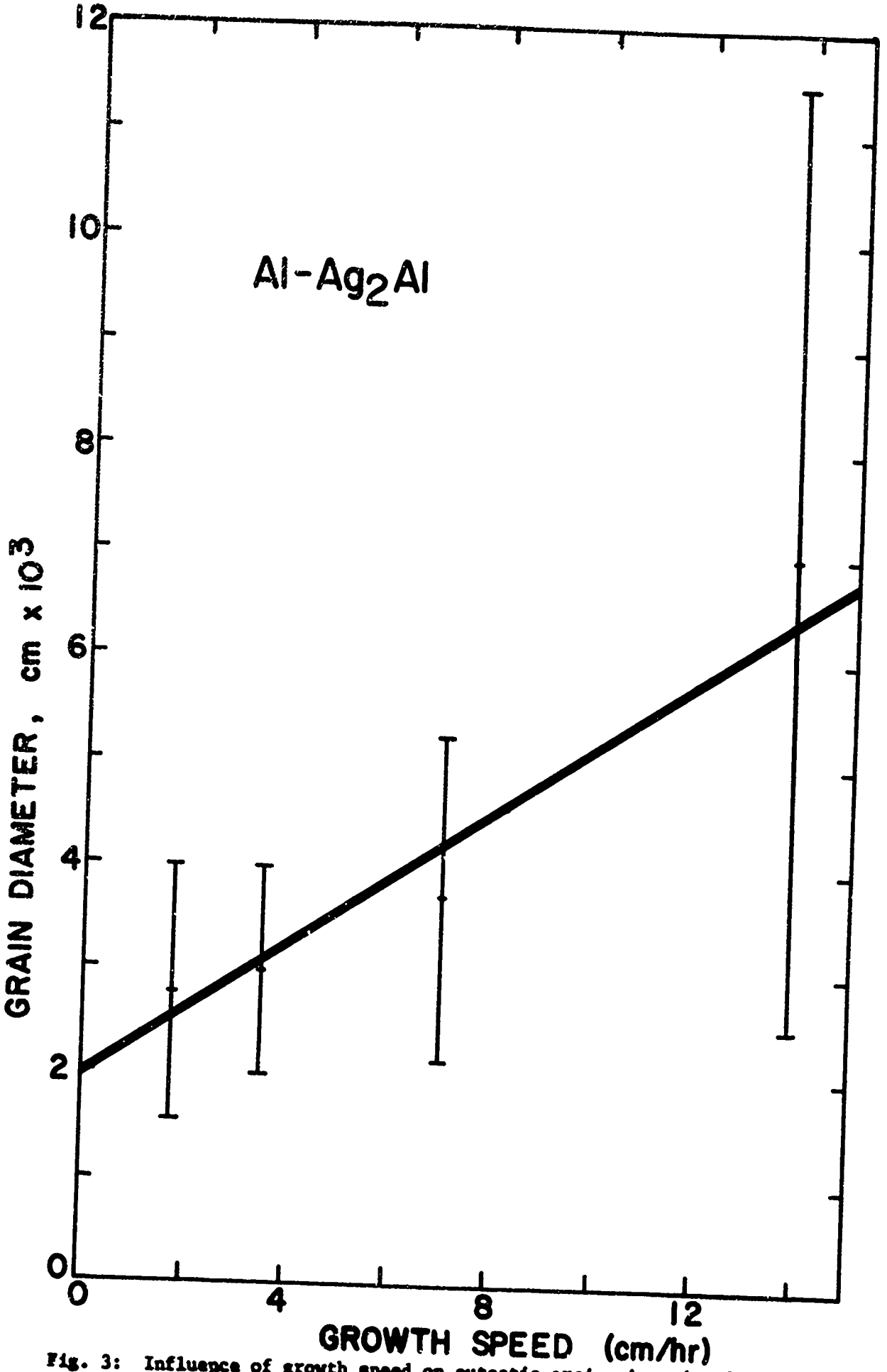

Fig. 3: Influence of growth speed on eutectic grain size, d, of Al-Ag_2Al. Bands denote scatter at each speed.

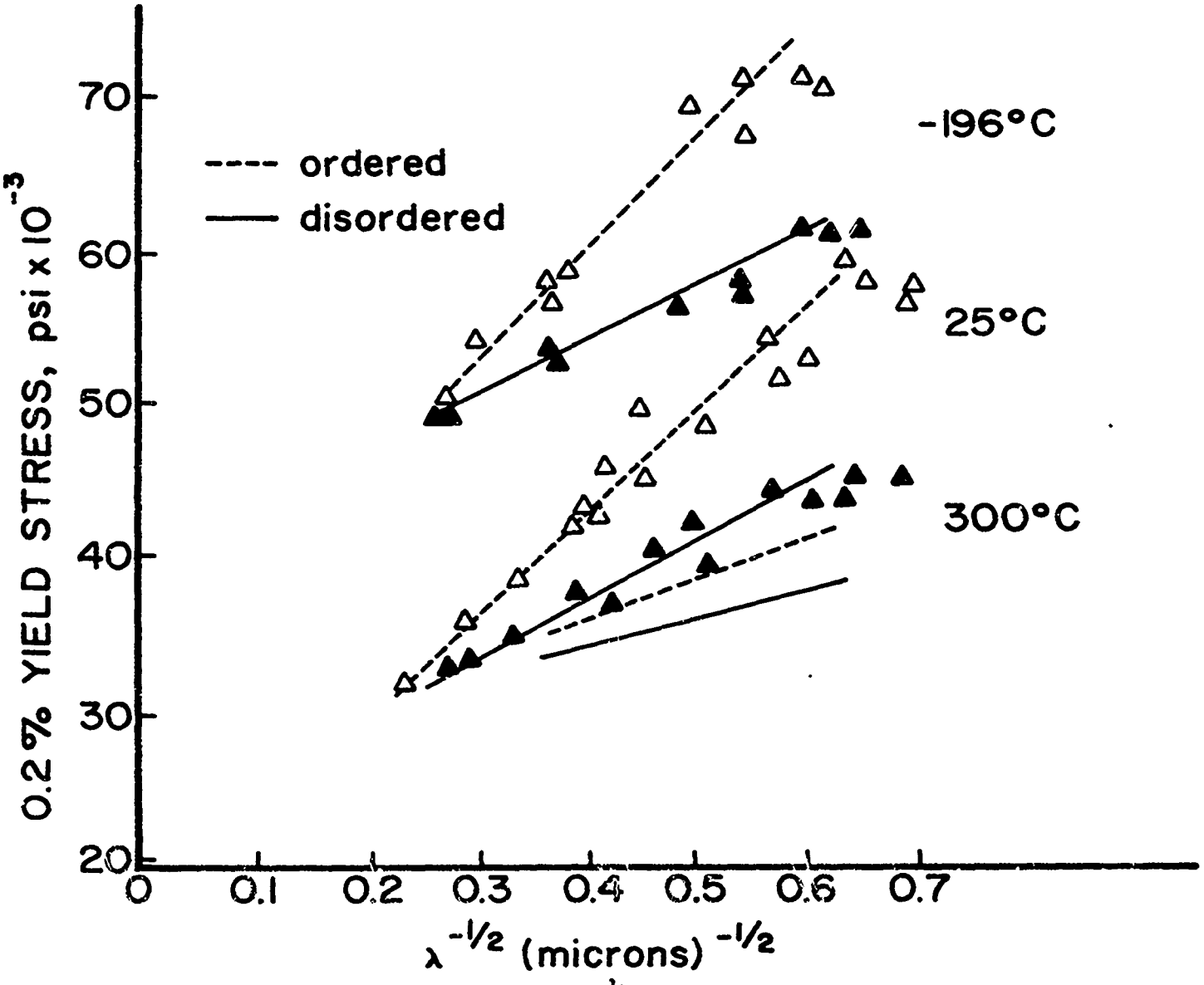

Fig. 4: Dependence of yield stress on $\lambda^{-\frac{1}{2}}$ for ordered and disordered Ag_3Mg-AgMg at -196°C, 25°C and 300°C. (Points at 300°C omitted for clarity).

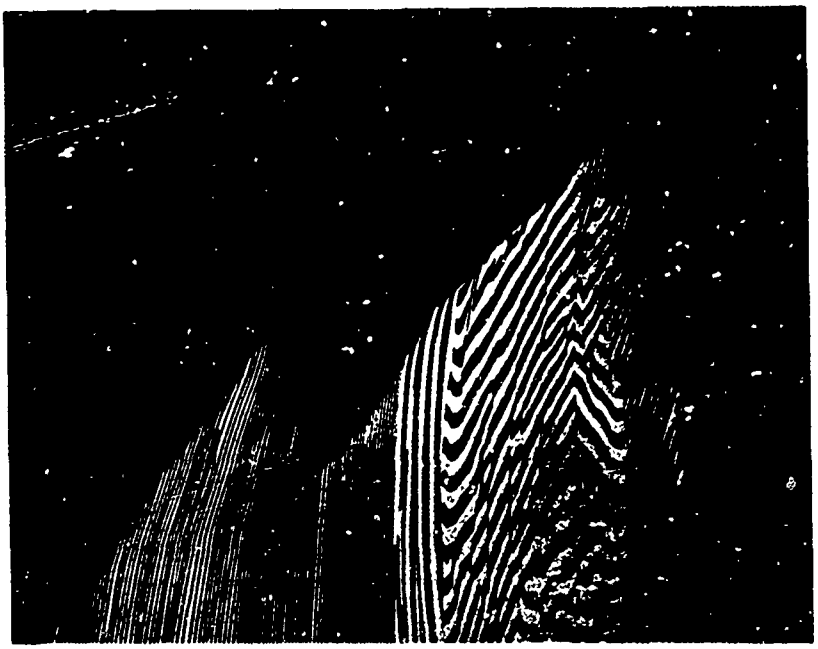

Fig. 5: Longitudinal section, showing crack path in ordered Ag_3Mg-AgMg, R = 3 cm/hr, tested at 25°C, x500.

(a)

(b)

(c)

Fig. 6: Electron fractographs of Ag_3Mg-AgMg,

a) SEM, ordered, R = 13.9 cm/hr, -196°C
G denotes eutectic grain boundary.
b) replica, disordered, R = 27.8 cm/hr, 25°C
c) replica, ordered, R = 27.8 cm/hr, 25°C

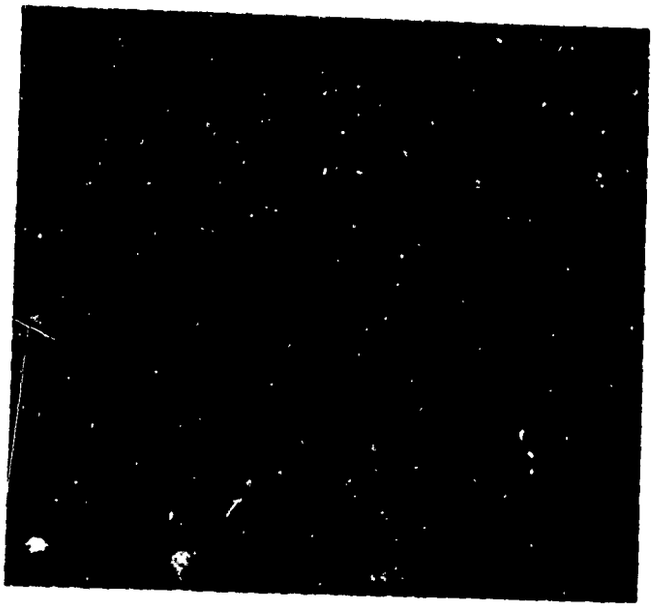

(a)

(b)

(c)

Fig. 6: Electron fractographs of Ag_3Mg-AgMg,

a) SEM, ordered, R = 13.9 cm/hr, -196°C
G denotes eutectic grain boundary.
b) replica, disordered, R = 27.8 cm/hr, 25°C
c) replica, ordered, R = 27.8 cm/hr, 25°C

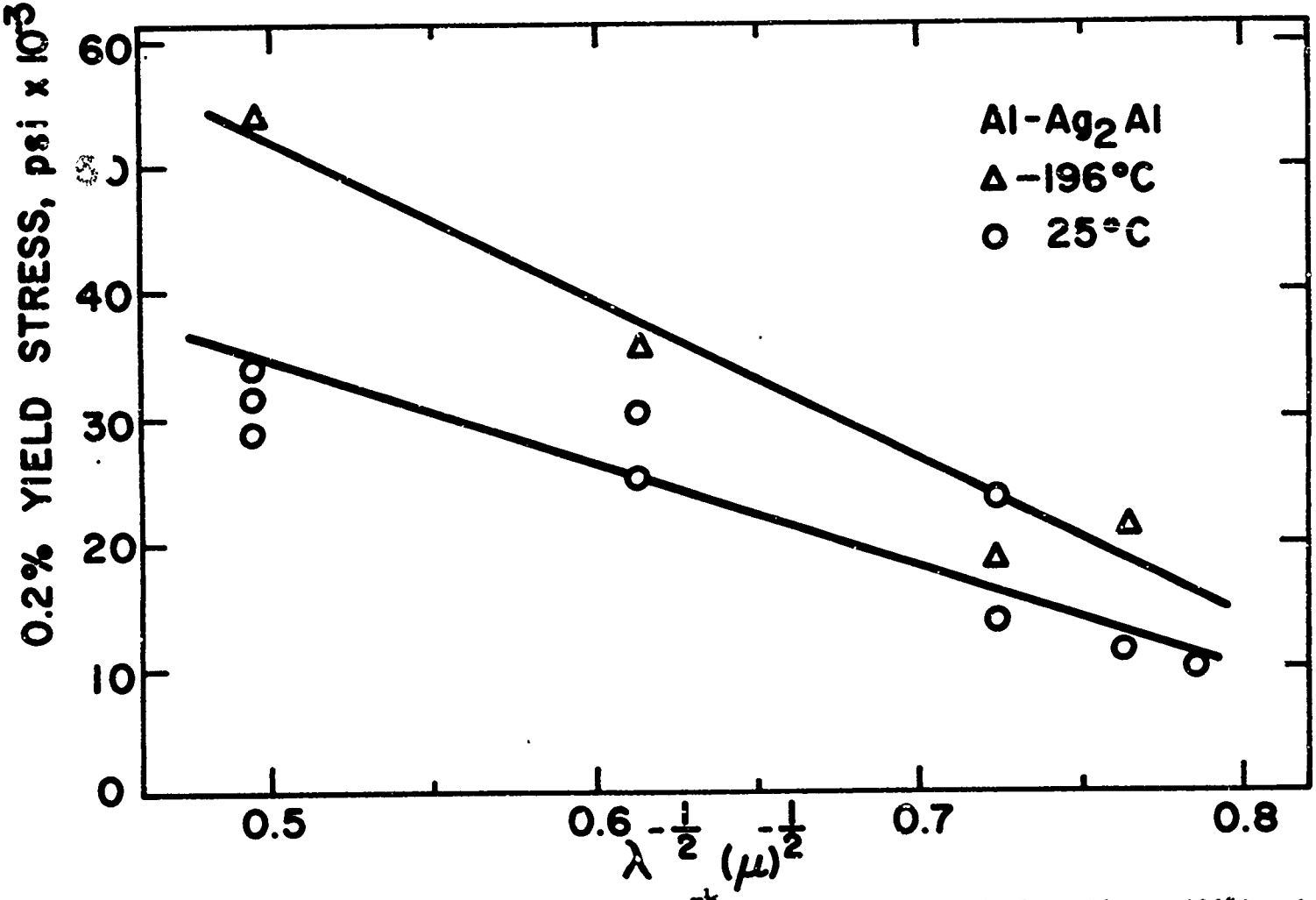

Fig. 7: Dependence of yield stress on $\lambda^{-\frac{1}{2}}$ for stress-relieved Al-Ag_2Al at -196°C and 25°C.

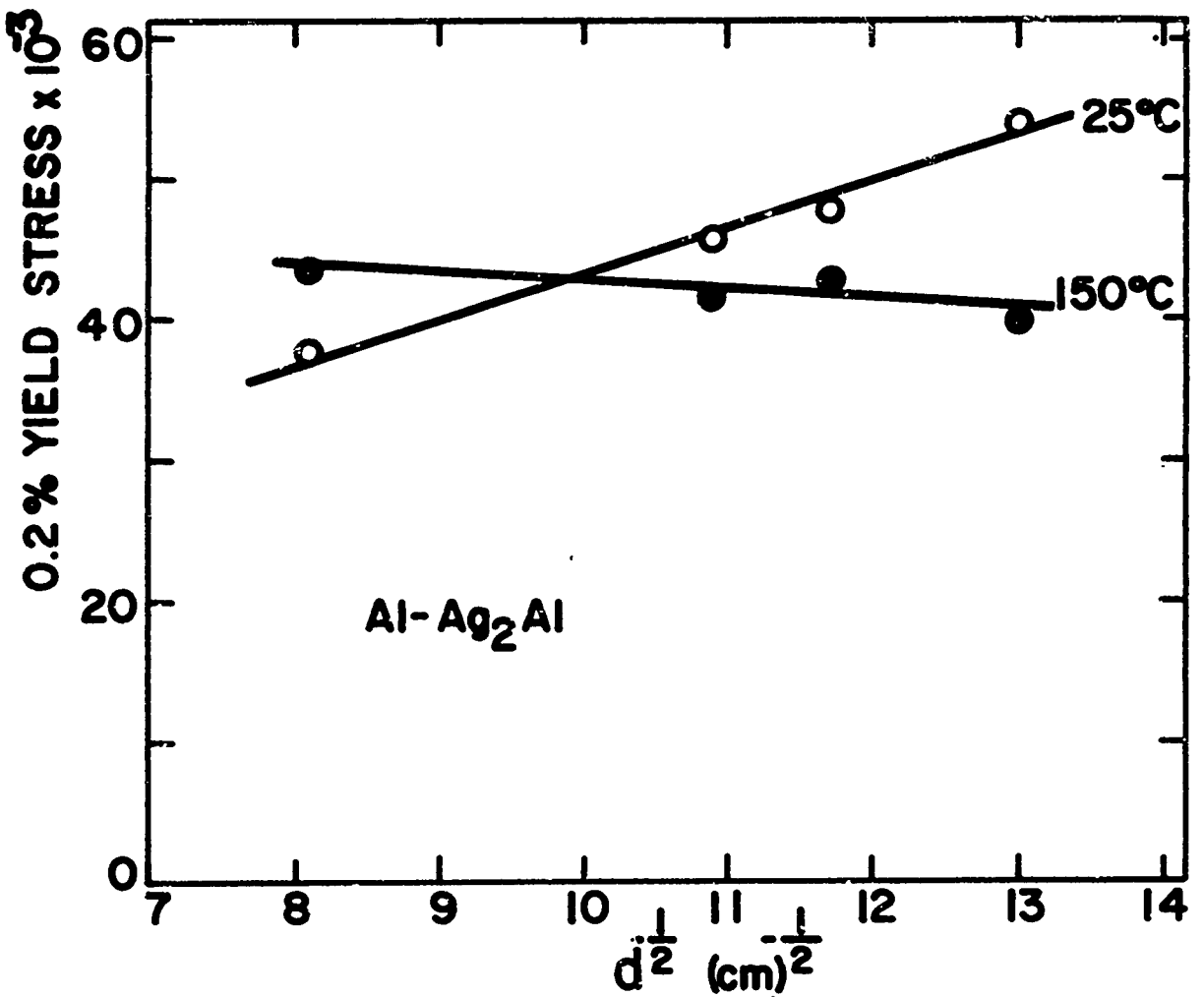

Fig. 8: Dependence of yield stress on $d^{-\frac{1}{2}}$ for stress-relieved Al-Ag_2Al at 25°C and 150°C.

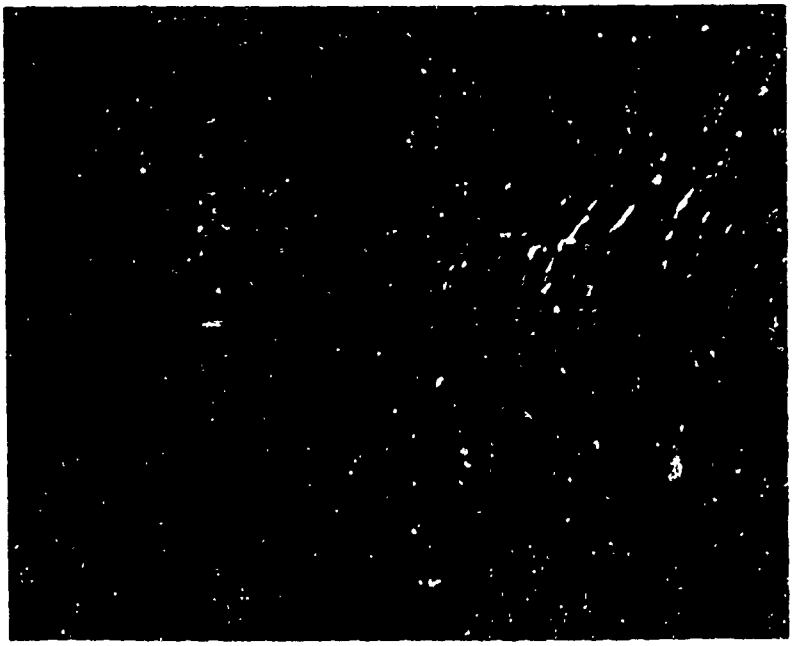

Fig. 9: Slip bands in Al-Ag_2Al, R = 6.9 cm/hr, x750.
Note traces terminate at grain boundaries, G.

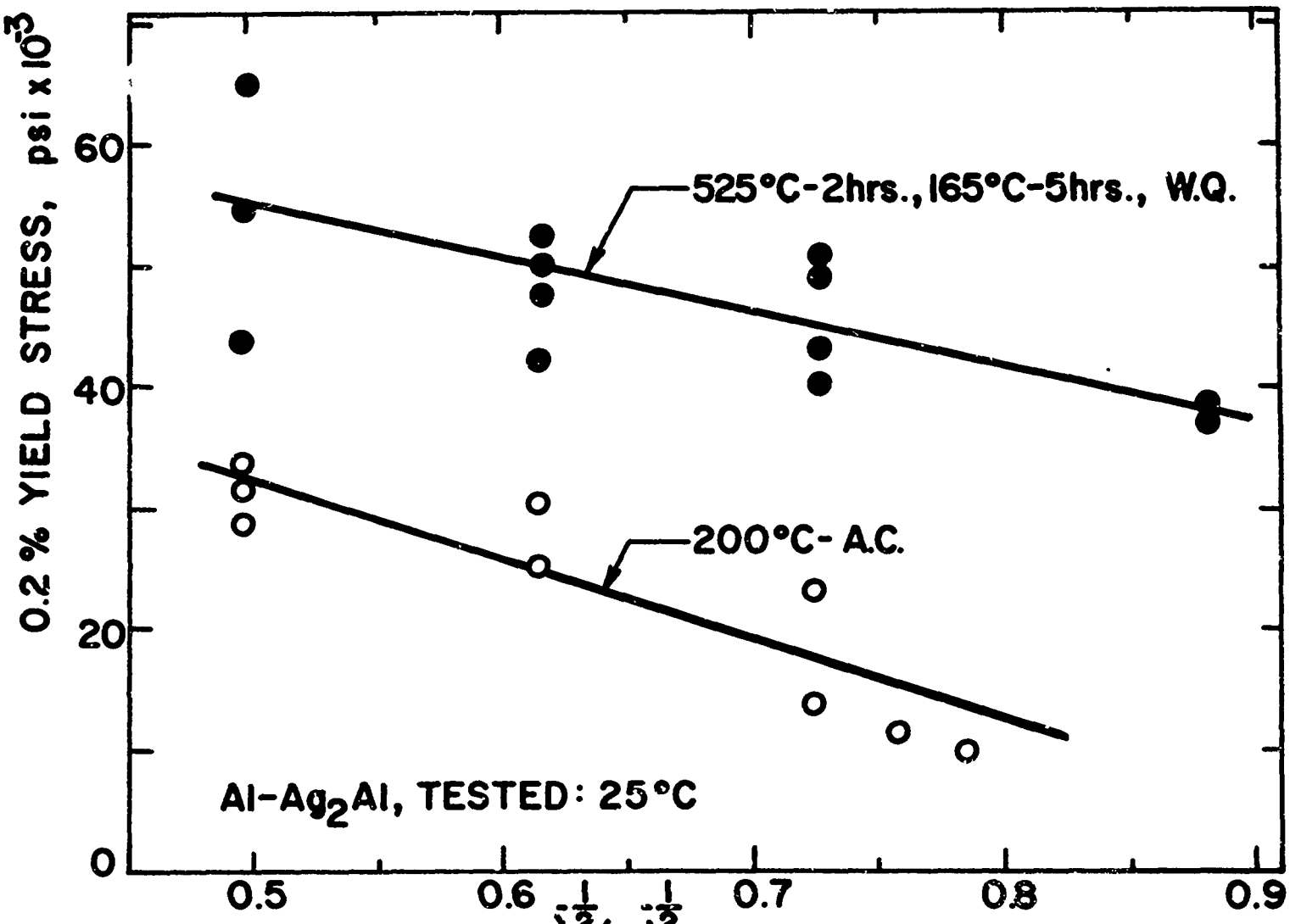

Fig. 10: Effect of aging heat treatment on the yield strength of Al-Ag_2Al.

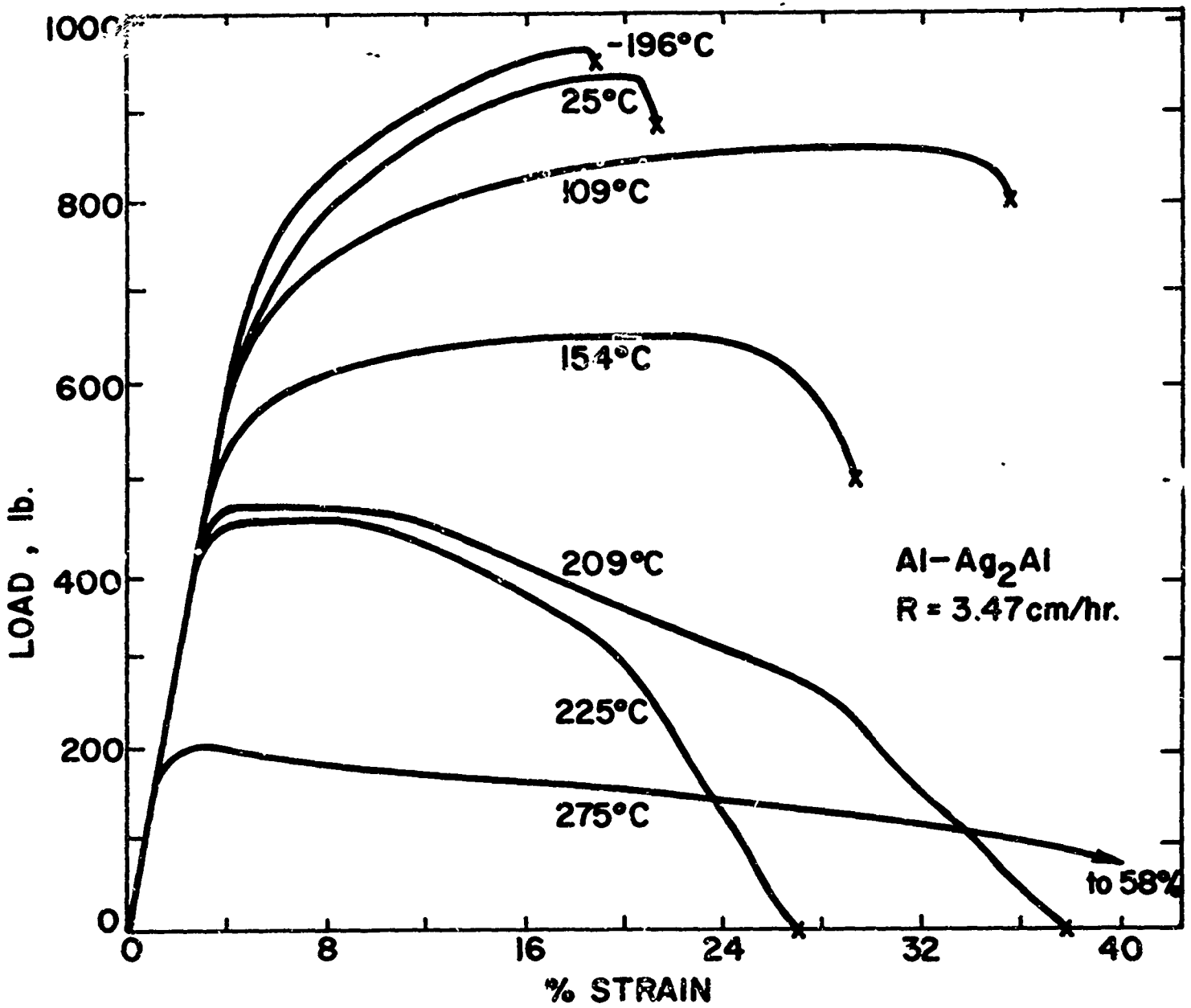

Fig. 11: Tensile properties of aged Al-Ag_2Al a) Load-strain curves at several test temperatures.

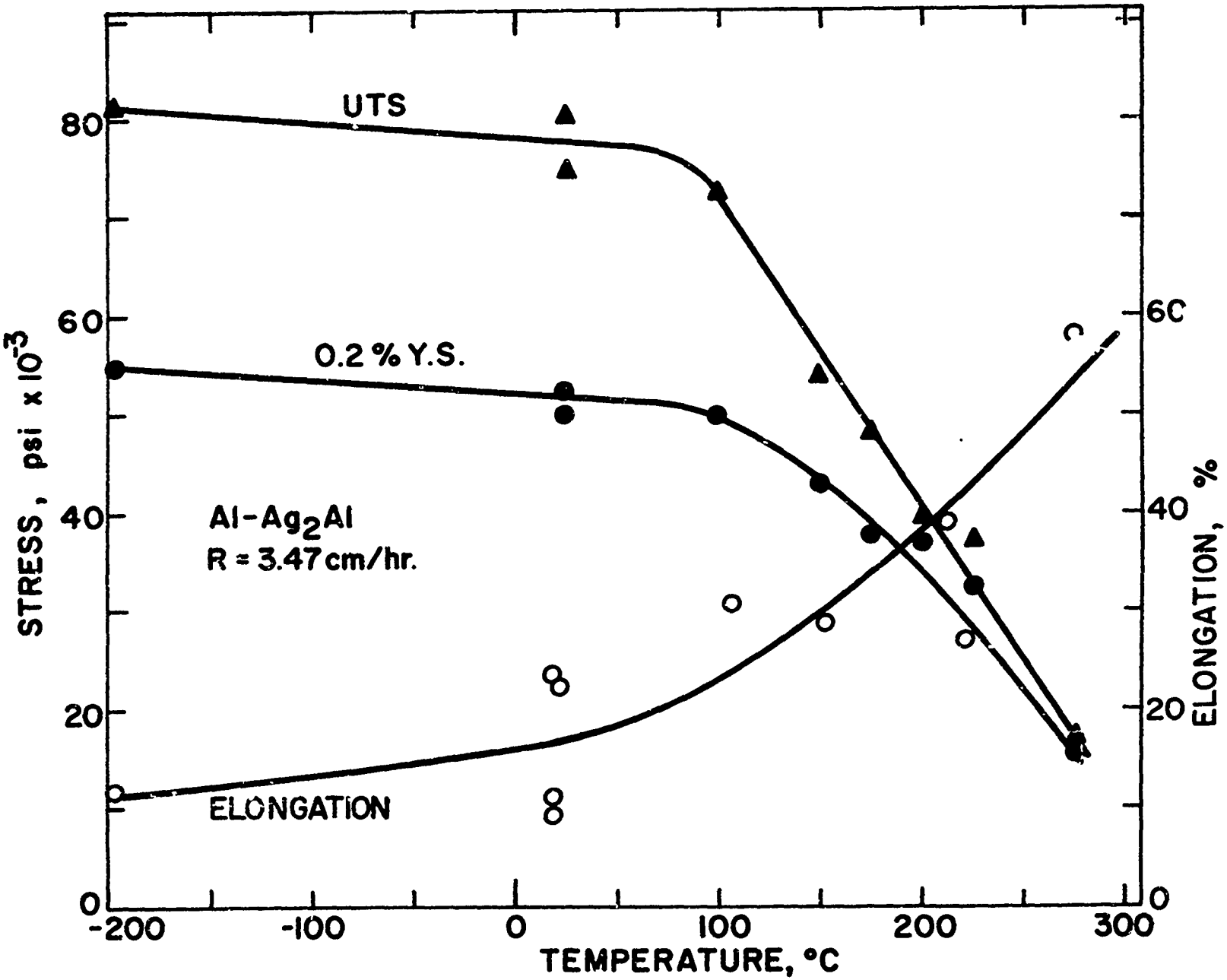

Fig. 11: Tensile properties of aged Al-Ag_2Al b) Influence of temperature on strength and ductility.

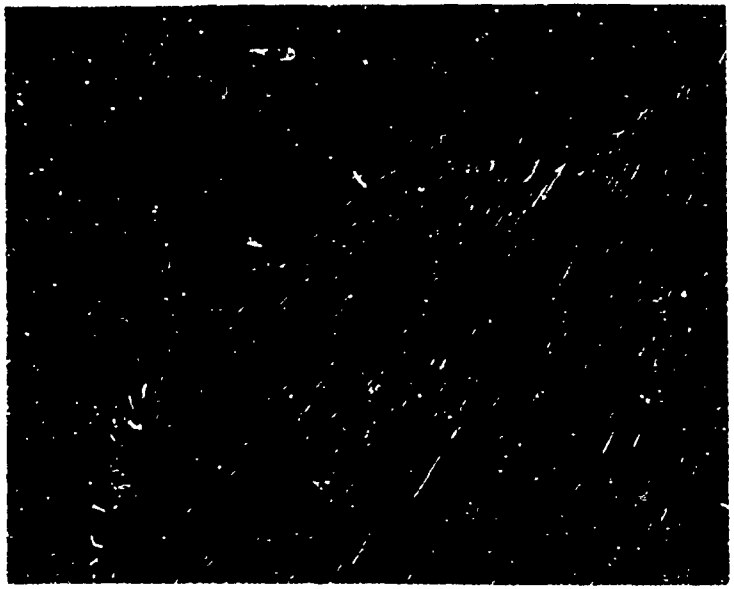

(a)

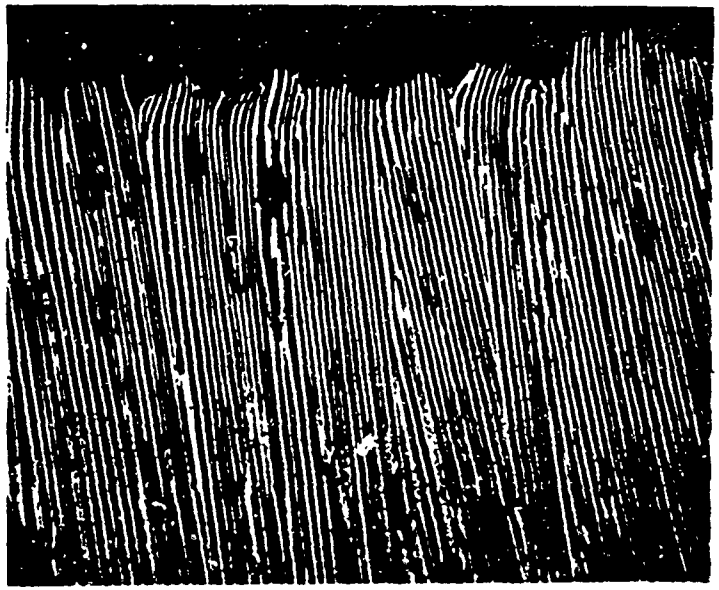

(b)

25

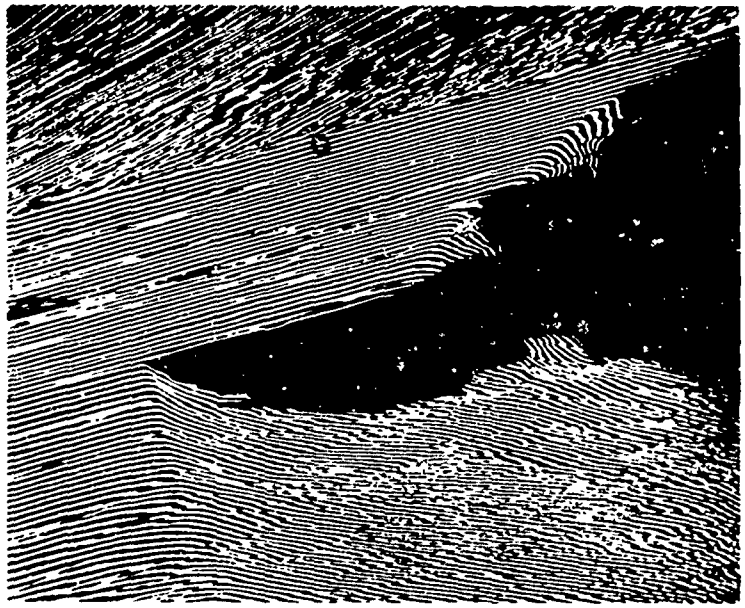

(c)

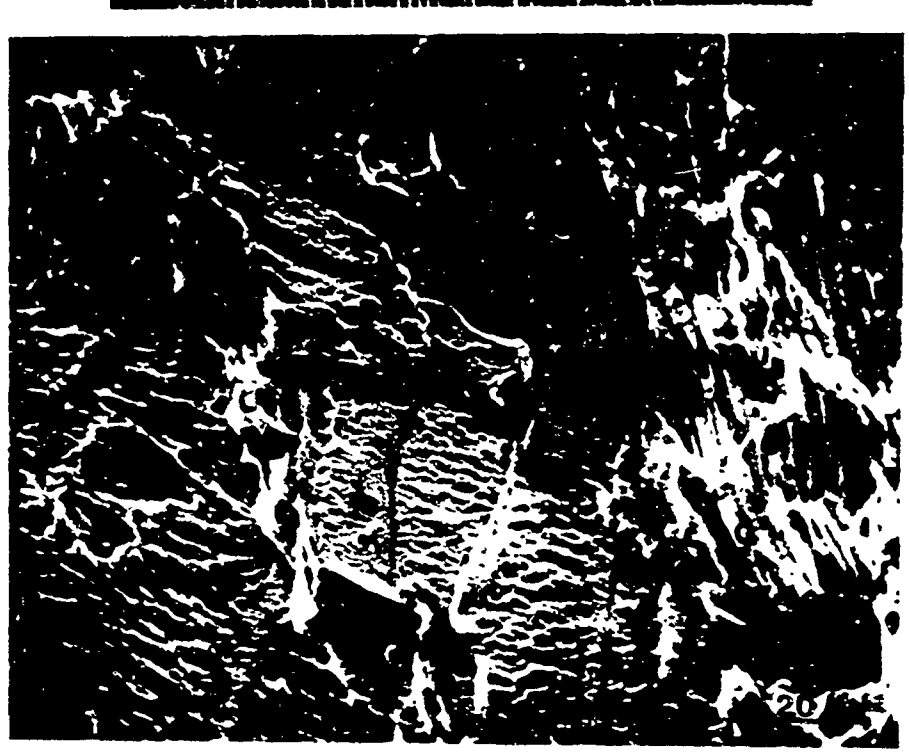

(d)

Fig. 12: Fracture modes in Al-Ag_2Al, with eutectic grain boundaries marked G.
(a) Crack path, -196°C, R = 31.7 cm/hr, x121
(b) Lamellae fractures, -196°C, R = 3.5 cm/hr, x500
(c) Interlamellar crack, -196°C, R = 6.9 cm/hr, x250
(d) SEM fractograph, -196°C, R = 3.5 cm/hr, x725